Essential Ingredients of a Method for Low Reynolds-Number Airfoils

Tuncer Cebeci*
California State University, Long Beach, California

A calculation method for low-Reynolds-number flows is described and appraised in terms of comparisons between calculations and measurements. It comprises interaction between solutions of inviscid- and boundary-layer equations and involves the e^n method to determine the location of the onset of transition with further interaction to insure that upstream effects of the turbulent-flow region are correctly represented. The importance of the length of the transition region, which usually occurs within a separation bubble, is demonstrated, and an extended version of the intermittency expression used in the Cebeci-Smith algebraic, eddy-viscosity formulation is proposed and shown to represent the separation-induced transitional flows. The comparison of calculated and measured results encompasses five airfoils, chord Reynolds numbers from 3×10^5 to 8×10^6, and angles of attack from 0–11 deg, and shows that the essential features of these flows are correctly represented.

I. Introduction

THE flows over airfoils at Reynolds numbers between 10^5 and 10^6 involve laminar, transitional, and turbulent boundary layers often with extensive regions of separated flow and always with a transition region that exists over a larger proportion of the chord than at higher Reynolds numbers. They are important to a range of applications including remotely piloted vehicles and helicopter rotors and emphasize the phenomena of transition, which has always proved difficult to represent although it is an essential requirement of extrapolation of wind-tunnel experiments to flight conditions. This paper is concerned with the calculation of flows of this type and, therefore, with identifying, assembling, and testing the components of the required procedure.

The solution of two-dimensional equations for inviscid flows and for boundary-layer flows can be achieved by a number of procedures, and the calculations reported here made use of the conformal-mapping method of Halsey[1] to solve the former with the finite-difference method described by Cebeci and Bradshaw[2] to solve the latter. The need to include the wake as part of the calculation at higher angles of attack has been demonstrated by Cebeci et al.[3], who also showed that interaction between the inviscid- and viscous-flow solutions was necessary at the higher angles of attack and at any angle where separated flow existed. As a consequence, the interactive boundary-layer approach described in Ref. 3 is also used here.

The importance of transition from laminar to turbulent flow is well known though the understanding to support its prediction is less secure. Investigations have ranged from fundamental studies of Tollmien-Schlichting waves to the development of empirical correlations where, for example, transition is presumed to take place at a specific Reynolds number. Examples of correlation formulas, based on measurements in two-dimensional, incompressible flows include those of Michel[4] and Granville[5] and the former, for example, assumes that transition occurs where the local Reynolds number based on the momentum thickness R_θ is related to length Reynolds number R_x by the equation

$$R_\theta = 1.174\left(1+\frac{22{,}400}{R_x}\right)R_x^{0.46} \tag{1}$$

There are also several empirical formulas for predicting the onset of transition in flows involving separation bubbles such as those given by Horton[6] and Crimi and Reeves.[7] The latter assumes that transition occurs when

$$\frac{y_{u=0}}{\delta_s^*} = \frac{10^6}{(u_e\delta^*/\nu)_s^2} \tag{2}$$

where $y_{u=0}$ denotes the distance from the wall and subscript s denotes separation. The problem of predicting transition within a separation bubble is difficult, and attempts have included the assumption that transition and separation coincide as well as empirical correlations such as that of Eq. (2). This correlation-type approach is clearly limited by its inability to take account of many of the parameters that are known to influence transition, including pressure gradients, heat transfer, roughness, surface curvature, and freestream turbulence.

A more general approach to the onset of transition is that proposed independently by Smith[8] and Van Ingen[9] and based on a linear-stability theory. It assumes that transition starts when a small disturbance is introduced at a critical Reynolds number and is amplified by a factor of e^9 or about 8×10^3: the effect of freestream turbulence can be represented by

$$n = -8.43 - 2.4\ell nT \tag{3}$$

where

$$T = \sqrt{u'^2}/u_e$$

as proposed by Mack.[10] The amplitude at a fixed point is independent of time and the spatial theory provides the required amplitude change.

The e^n method is used in the present calculations to represent the onset of transition since its accuracy has been studied extensively for two-dimensional and axisymmetric bodies with and without heat transfer. For example, Wazzan[11] has pre-

Received Aug. 22, 1988; revision received March 7, 1989.

*Professor and Chairman, Aerospace Engineering Department. Fellow AIAA.

sented a substantial review which shows that the method provides values of transition in good agreement with experiment. In flows with separation, however, there has been less activity and Nayfeh et al.[12] have reported one of the few attempts to apply the method, which they did in the context of the corrugated-plate flows of Fage.[13] Cebeci and Egan[14] have addressed the same problem with detailed differences in the application of the e^n method and have provided results which suggest that the method can represent the effects of separation on the location of transition in a manner which can be used for the present purpose. It is clear, however, that the region of transitional and turbulent flow, especially where separation exists, must be adequately predicted, and its consequences for the location of the onset of transition must be incorporated by an additional iterative process to determine a converged transition location.

The turbulence model used to represent the Reynolds stresses in the region of turbulent flow is that of Cebeci and Smith[15] and was chosen because of its simplicity and known range of applicability. It has also been shown, for example by Chang et al.[16] and Cebeci et al.,[17] that for external boundary-layer flows, there is little to be gained from the use of higher-order models. The application of this model to transitional flow is achieved with the help of an intermittency factor, which is further considered in this paper to permit its applicability to transitional regions within separation bubbles.

Since the individual elements of the calculation method have been described previously, the descriptions of the following two sections are brief. As part of the interactive boundary-layer procedure of Sec. II, the transitional model is considered and described. The e^n method of Sec. III forms part of a further interactive calculation, this time to insure that location of the onset of transition is consistent with the inviscid and boundary-layer flows. The implementation of the overall procedure and the computer requirements are discussed briefly in this third section. Calculated results are presented in Sec. IV and correspond to the experimental configurations of Gault,[18] Cousteix and Pailhas,[19] Hoheisel et al.,[20] Liebeck and Camacho,[21] and Render et al.[22] The emphasis of Sec. IV is an appraisal of the calculation method, and this is achieved by comparing the two sets of results and examining the magnitudes and reasons for discrepancies. The paper ends with a summary of the more important findings and with a brief statement of their implications for future work.

II. Interactive Boundary-layer Method

The conformal mapping method used to solve the two-dimensional, inviscid-flow equations involves transformation of the region outside of the airfoil to the region outside of a unit circle and solution of the resulting equations in the transformed plane. The transformation was achieved in a sequence of three conformal mappings and the solutions of the transformed equations made use of Fourier-analysis techniques discussed in Ref. 1. It was necessary to involve the wake at higher angles of attack, and the dividing streamline was computed by conformal mapping as a line of constant stream function.[3]

The boundary-layer calculation procedure represents the wall flow, with its possible regions of separation, and the downstream wake. The boundary-layer equations were solved in inverse form to avoid the singularity at separation and the convective term $u(\partial u/\partial x)$ set to zero in regions of negative streamwise velocity. This approximation, suggested by Reyher and Flügge-Lotz[23] and often referred to as the FLARE approximation, was needed to avoid numerical instabilities due to negative u velocity. In the inverse procedure, the relationship between the inviscid and viscous flows was established by the interaction formula for the edge velocity, as described by Veldman[24] and Cebeci et al.[25] The calculations started by computing the pressure distribution on the airfoil and in the wake in the absence of viscous effects. Next, the displacement thickness resulting from this pressure distribution was obtained from the solution of the boundary-layer equations with the calculations starting at the forward stagnation point and proceeding with laminar flow until the transition criteria imposed the eddy-viscosity formulation. The displacement thickness distribution resulting from these calculations was used to determine a blowing velocity distribution v_n by differentiating the product of external velocity and displacement thickness with respect to the surface distance s, that is

$$v_n = \frac{\mathrm{d}}{\mathrm{d}s}(u_e\delta^*) \tag{4}$$

so that the inviscid-flow equations were solved again subject to a new boundary condition. This process was repeated on an iterative basis until the solutions of both boundary-layer and inviscid-flow equations converged. The blowing velocity was also determined in the wake and required a further iteration to insure that the divided streamline was correctly located. Special care was required in the near wake to insure that step lengths were sufficiently small so as to avoid convergence problems.

The turbulence model of Cebeci and Smith[15] comprises an algebraic eddy-viscosity formulation that employs a mixing length approach to the inner layer and a constant eddy viscosity for the outer layer. The model's ability to represent turbulent wall-boundary layers and wakes is well documented, for example, in Refs. 15-17. The transition region is represented by an expression suggested by Chen and Thyson,[26] which multiplies the inner and outer eddy-viscosity formulas. It is given by

$$\gamma_{tr} = 1 - \exp\left[-G(x - x_{tr})\int_{x_{tr}}^{x}\frac{\mathrm{d}x}{u_e}\right] \tag{5}$$

Here x_{tr} is the location of the beginning of transition and G is defined by

$$G = \left(\frac{3}{C^2}\right)\frac{u_e^3}{\nu^2}R_{x_{tr}}^{-1.34} \tag{6}$$

where the transition Reynolds number $R_{x_{tr}} = (u_e x/\nu)_{tr}$, and C is constant with a recommended value of 60. According to Eq. (5), the extent of the transition region $R_{\Delta x}$ is related to the transition Reynolds number $R_{x_{tr}}$ by

$$R_{\Delta x} = CR_{x_{tr}}^{2/3} \tag{7}$$

This expression was obtained from data based on attached flows and it is likely to be less applicable to flows with separation.

Experiments show that the extent of a separation bubble and the location of transition depend on the Reynolds number. At high Reynolds numbers, transition usually corresponds to the

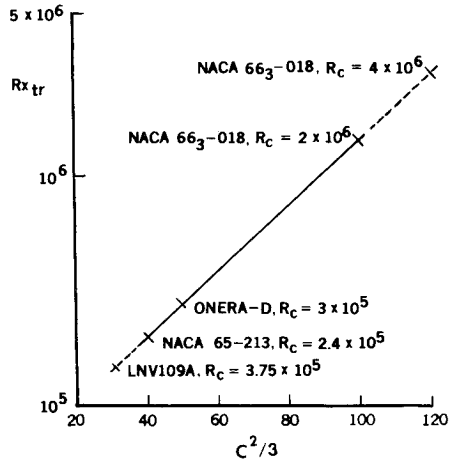

Fig. 1 Variation of $C^2/3$ with transition Reynolds number. $R_{x_{tr}}(\equiv u_e x/\nu)$

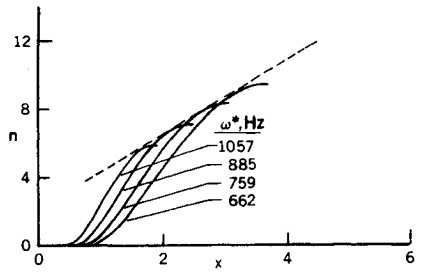

Fig. 2 Variation of the amplification factors with distance and frequency for Blasius flow.

location of separation, and the length of the bubble is relatively short. At low Reynolds numbers, transition can occur inside the bubble and can strongly influence the nature of flow. To take account of the corresponding effects, a correlation formula was devised to represent C of Eq. (7) in terms of $R_{x_{tr}}$ and based on experimental data, which show separation induced transition at low Reynolds numbers. This correlation formula is shown in Fig. 1 together with the experimental data of Refs. 18-21 obtained for airfoils NACA 66_3-018, ONERA-D, NACA 65-213, and LNV109A, respectively. The data encompasses a typical low Reynolds number range from $R_c = 2.4\times 10^5$ to 2×10^6, falls conveniently on a straight line on a semilog scale, and can be represented by the equation

$$C^2 = 213(\log R_{x_{tr}} - 4.7323) \tag{8}$$

Care should be taken in the use of Eq. (8) outside the range of experiments, particularly at high Reynolds numbers where the separation bubble is likely to be small and a limiting value of $C = 60$ applies.

The application of the above calculation procedure requires the location of the onset of transition, and the following section describes how this was obtained and used.

III. Linear Stability and the e^n Method

In the e^n method, the laminar boundary-layer equations are solved first for a given pressure distribution, and the velocity profiles are calculated as a function of surface distance along the body. Next, the stability equation, known as the Orr-Sommerfeld equation

$$\phi^{iv} - 2\alpha^2\phi'' + \alpha^4\phi - iR(\alpha u - \omega)(\phi'' - \alpha^2\phi) + iR\alpha u''\phi = 0 \tag{9}$$

and its boundary conditions with D denoting $\mathrm{d}/\mathrm{d}y$, subscript e the "edge" conditions, and ξ_2 defined by $\xi_2^2 = \alpha^2 + iR(\alpha u_e - \omega)$

$$\bar{y} = 0, \qquad \phi = \phi' = 0 \tag{10a}$$

$$\bar{y} = \bar{\delta}, \qquad (D^2 - \alpha^2)\phi + (\alpha + \xi_2)(D + \alpha)\phi = 0$$

$$(D + \xi_2)(D^2 - \alpha^2)\phi = 0 \tag{10b}$$

are solved,[2] and the stability properties of the velocity profiles u and u'' are examined. Equations (9) and (10) have been written in dimensionless form so that all velocities and lengths are normalized by a reference velocity u_0 and length ℓ so that the Reynolds number R is defined by $R = u_0\ell/\nu$. The radian frequency ω is made dimensionless by dividing the physical frequency ω^* by u_0/ℓ. Primes denote differentiation with respect to a dimensionless distance $\bar{y}(\equiv y/\ell)$. The wavelength α, which is complex ($\equiv \alpha_r + i\alpha_i$), has also been normalized by the reference length ℓ.

In the e^n method, the onset of transition is computed by evaluating the integral

$$n = \int_{x_0}^{x} -\alpha_i \mathrm{d}x \tag{11}$$

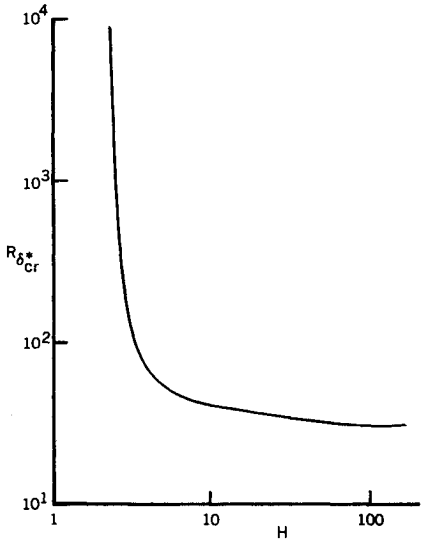

Fig. 3 Variation of the critical Reynolds number based on displacement thickness $R_{\delta^*_{cr}}$ with shape factor for Falkner-Skan flows.

for a set of specified dimensional frequencies ω^*. Here α_i represents the amplification rates determined from Eq. (9) using velocity profiles and their second derivatives obtained from the interactive boundary-layer procedure of Sec. II. The solution of Eq. (9) begins at a Reynolds number greater than the critical value, R_{cr}, on the lower branch of the neutral stability curve. This provides the desired frequency which, at the subsequent Reynolds numbers, allows the solution of the eigenvalue problem in terms of α and to the amplification curves of Fig. 2. The process is repeated to obtain similar amplification curves for different values of ω^*. As can be seen from Fig. 2, the envelope of the resulting curves corresponds to the maximum amplification factors from which transition is computed by assuming a value for n, commonly taken to be between 8 and 9.

The numerical method used to solve the Orr-Sommerfeld equation, Eq. (9), and its boundary conditions, Eq. (10), also makes use of Keller's box scheme and is described in Cebeci and Bradshaw[2] for attached flows. The eigenvalue procedure, however, is implemented to extend the scheme to separated flows by the use of a continuation method[14] in which the velocity profiles u and u'' under consideration at a Reynolds number of R are defined by

$$u = u_{\mathrm{ref}} + n(u - u_{\mathrm{ref}}) \qquad u'' = u''_{\mathrm{ref}} + n(u'' - u''_{\mathrm{ref}}) \tag{12}$$

Here u_{ref} and u''_{ref} denote reference profiles at a Reynolds number of R_{ref} and have eigenvalues α_0 and ω_0. The parameter n is a sequence of specified numbers ranging from 0-1. It follows from Eq. (12) that for $n = 0$, the profiles u and u'' correspond to the reference profiles and for $n = 1$, to those with eigenvalues of α and ω which are unknown.

The stability-transition calculations for an airfoil flow were started by first obtaining the solutions of the laminar boundary layers with the interactive method of the previous section. Since an inverse procedure was being used, the solutions included flows with or without separation. The stability calculations were then initiated at the first x station where the Reynolds number based on the displacement thickness, $R_{\delta^*}(\equiv u_e\delta^*/\nu)$, exceeded the $R_{\delta^*_{cr}}$ established for similar boundary layers (see Fig. 3). Several dimensional frequencies at different x locations were then computed on the lower branch of the neutral stability curve in order to determine the amplification rates, $\alpha_i(x)$. In regions of no flow separation, the eigenvalue procedure described in Ref. 2 operated satisfactorily and did not require the continuation method. In regions

of flow separation, however, this was not the case, and the velocity profiles u and u'' at R were found to be rather sensitive to the initial estimates of the eigenvalues for α. With the use of the continuation method with reference velocity profiles corresponding to those of a previous x station and with increments of Δn around 0.1, the sensitivity vanished, and the eigenvalues were computed satisfactorily as in attached flows.

As was discussed by Cebeci and Egan,[14] the envelope procedure used in the e^n method, which allows the dimensional critical frequency to be determined indirectly and conveniently, is not applicable to flows with separation. It is necessary to search for this frequency in the calculations. The results to be presented in Sec. IV indicate that in some cases the amplification rates were sensitive to the dimensional frequencies computed on the neutral stability curve and was necessary to take relatively small Δx increments on the airfoil.

Once the onset of transition location was computed, the remaining portion of the flow on the airfoil and in the wake which involved transitional and turbulent flows was computed by the interactive boundary-layer scheme of Sec. II. Several sweeps were performed for this transition location and for the inviscid pressure distribution until the solutions converged. A new inviscid pressure distribution which made use of the boundary-layer solutions through the use of the blowing velocity was computed in order to again obtain laminar boundary-layer solutions on the airfoil to predict the onset of transition and their subsequent transitional and turbulent-flow calculations on the airfoil and in the wake until convergence. The results obtained in this way are presented in Sec. IV and indicate that in general this procedure, which involved the calculation of transition by the e^n method and the calculation of inviscid and viscous flows, required three to four iterations.

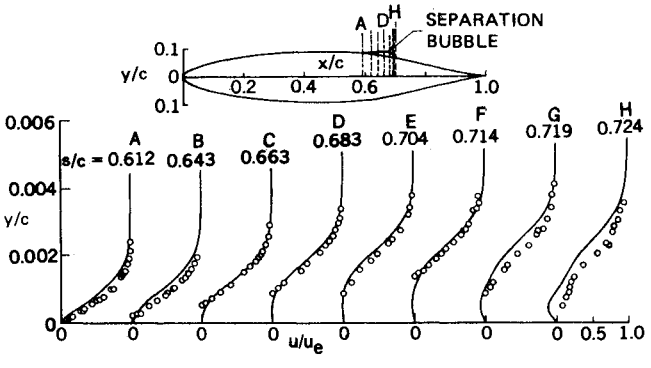

Fig. 4 Comparison of calculated (solid lines) and measured (symbols) velocity profiles for NACA 663-018 airfoil for $\alpha = 0$ deg, $R_c = 2 \times 10^6$.

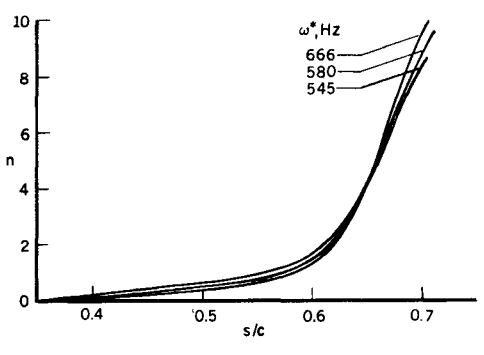

Fig. 5 Variation of amplification rates on the upper surface of the NACA 663-018 airfoil at different frequencies for $\alpha = 0$ deg, $R_c = 2 \times 10^6$.

IV. Results and Discussion

The calculation method described in Secs. II and III appears to contain the essential ingredients for an accurate predictive procedure. It involves approximations consequent upon the use of time-averaged, boundary-layer equations and in the determination of the transition location and presumes that a comparatively simple model is sufficient to represent turbulent wall flows and wakes. An assessment of the consequences of these assumptions requires consideration of experimental data which is itself subject to assumptions including the extent of two-dimensionality of the mean flow and the influence of wind-tunnel characteristics on the nature and extent of separation bubbles. Thus, a definitive assessment of the accuracy of predicted flow properties is not likely to be possible, and a decision as to the viability of the method to represent trends correctly and to provide a basis for design requires comparison of calculated results with an extensive range of acceptable experiments. The following paragraphs describe flow configurations investigated experimentally in

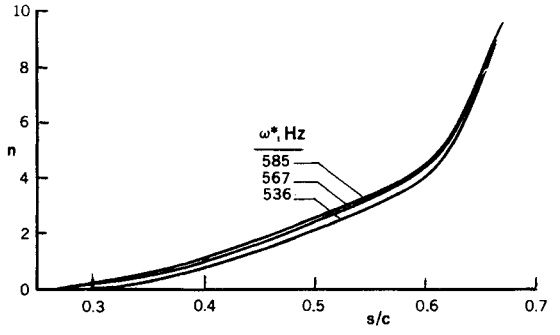

Fig. 6 Variation of amplification rates on the upper surface of the NACA 663-018 airfoil at different frequencies for $\alpha = 2$ deg, $R_c = 2 \times 10^6$.

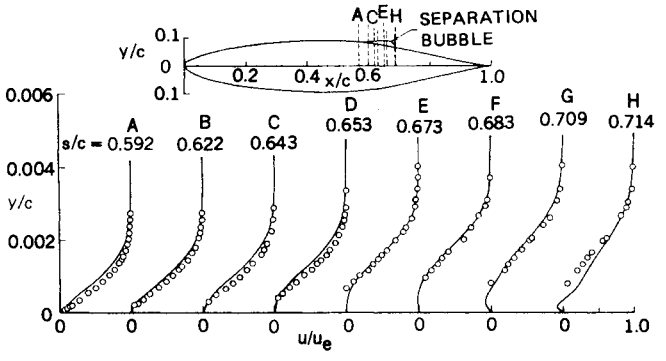

Fig. 7 Comparison of calculated (solid lines) and measured (symbols) velocity profiles for NACA 663-018 airfoil for $\alpha = 2$ deg, $R_c = 2 \times 10^6$.

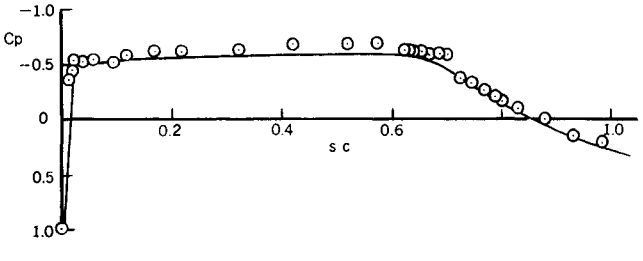

Fig. 8 Comparison of calculated (solid lines) and measured (symbols) pressure coefficients for NACA 663-018 airfoil for $\alpha = 2$ deg, $R_c = 2 \times 10^6$.

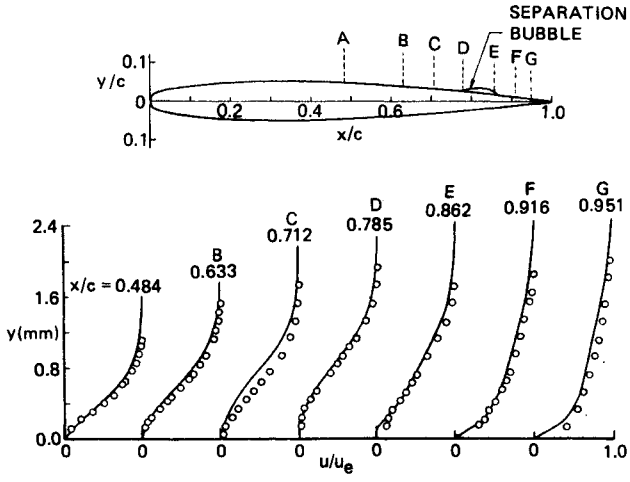

Fig. 9 Comparison of calculated (solid lines) and measured (symbols) velocity profiles for ONERA-D airfoil for $\alpha = 0$ deg, $R_c = 3 \times 10^5$.

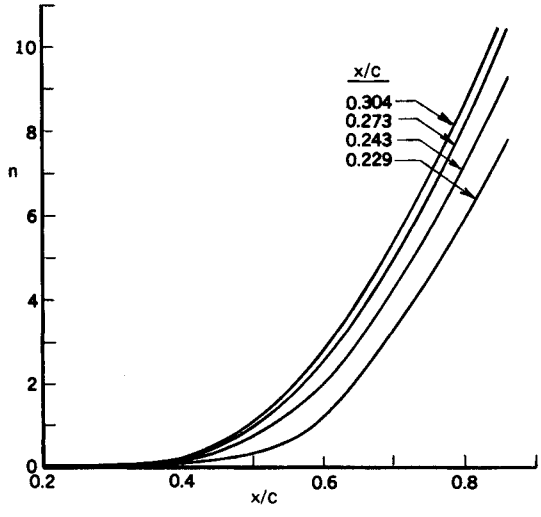

Fig. 10 Variation of amplification rates on the upper surface of the ONERA-D airfoil at different frequencies computed at four different chordwise locations.

five different research laboratories and encompassing airfoils, chord Reynolds numbers, R_c, and angles of attack, α, which are sufficient to insure that the relative importance of the interaction, transition location, and turbulence model is varied over a range, which is similar to that likely to be experienced in practice.

The experiments of Gault[18] were performed in the NASA Ames Research Center 7 × 10 ft wind tunnel with two airfoils, Reynolds numbers from 1.5–10 × 10^6, and angles of attack from 0–15 deg. Emphasis was placed on the NACA 66_3-018 airfoil at angles of attack of 0 and 2 deg for which detailed velocity information was provided through regions of separated flow which occurred near midchord. A main purpose was to identify locations of separation, transition, and reattachment, and with freestream turbulence intensities less than 0.2%, the flow might be expected to be reproducible. Figure 4 displays the NACA 66_3-018 airfoil together with measured and calculated mean-velocity profiles for zero angle of attack and for a chord Reynolds number of 2×10^6. Due to the presence of the separation bubble near midchord, the amplification rates were found to grow very fast in that region (see Fig. 5) and required a very fine spacing in the x direction in order to compute the eigenvalues. As can be seen from Fig. 5, the envelope procedure used in attached flows does not apply to

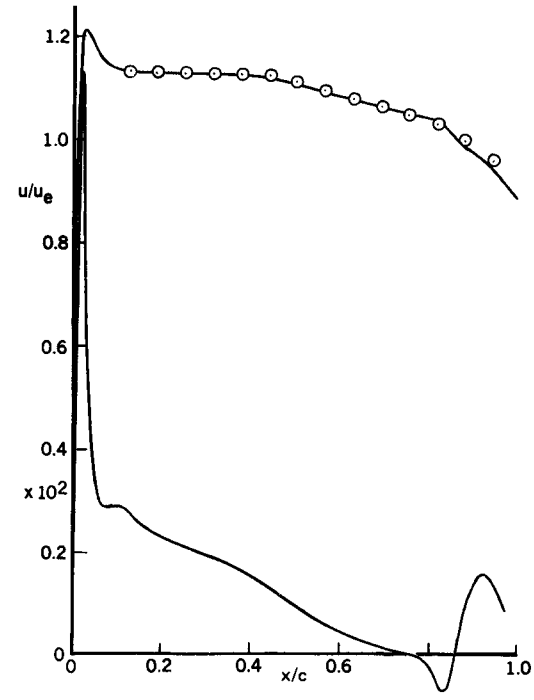

Fig. 11 Results for the upper surface of the ONERA-D airfoil. Symbols denote experimental data.

flows with separation. Furthermore, the amplification rates are not overly sensitive to the dimensional frequencies and with those computed at $s/c = 0.35$ and 0.40 they produce similar results due to the rapid growth in the separation region. At first transition was computed at a location close to the separation point ($s/c \simeq 0.62$) but moved inside the bubble in the second cycle. The experimental transition location was reported to be at $(s/c)_{tr} = 0.715$. The computed transition location was at $s/c = 0.685$ for $n = 8$ and $s/c = 0.693$ for $n = 9$. A value of $n = 10.6$ was required to match the experimental location. In all of the calculations reported here, the values of $n = 8$ was taken as in Ref. 14.

We should note that development of turbulence models for transitional flows, especially at low Reynolds numbers, is considerably more difficult than the task in high Reynolds number flows. This is because the transition location is part of the modeling task, and any errors in its computation can lead to inaccuracies in the turbulence model.

Figures 6–8 show the results for the same Reynolds number but for $\alpha = 2$ deg. As can be seen from Fig. 6, the amplification rates have the same behavior as those for $\alpha = 0$ deg in that they vary rapidly in the region of flow reversal, and they are not very sensitive to the choice of dimensional frequencies. In this case, the experimental transition location was at $s/c = 0.710$ in contrast to the computed values at $s/c = 0.66$ for $n = 8$, $s/c = 0.676$ for $n = 9$, and $n = 12.5$ for $s/c = 0.71$. The computed velocity profiles in Fig. 7 indicate good agreement with the experiment except near the trailing edge. The pressure coefficient results of Fig. 8 also indicate good agreement with data except near the separation bubble region where the calculations do not exhibit the relatively flat behavior in C_p.

The ONERA-D airfoil was examined by Cousteix and Pailhas[19] in a wind tunnel with a chord Reynolds number of 3×10^5 at zero angle of attack. The airfoil and mean-velocity profiles, variation of amplification rates, distributions of freestream velocity, skin-friction coefficient, and distributions of displacement momentum thicknesses are shown in Figs. 9–12. In this case, the measured and calculated results are in close agreement with appreciable differences only in the velocity profiles immediately upstream of boundary-layer separation where, as suggested for example by Thompson and Whitelaw[27] and Nakayama,[28] we might expect cross-stream pressure gradi-

ents and normal stresses to have a locally important role. In this case, transition occurred within the separated flow region and caused reattachment shortly thereafter. The calculations revealed transition at $x/c = 0.79$ for $n = 8$, at $x/c = 0.81$ for $n = 9$ in comparison with measurements which revealed transition at $x/c = 0.808$. We note from Fig. 12 that the agreement between calculated and experimental results at the trailing edge is not as good as the rest of the flow. This is believed to be due to the wake effect.

Hoheisel et al.[20] were also concerned with zero angle of attack, this time with a NACA 65-213 airfoil at a chord Reynolds number of 2.4×10^5 so that the flow was separated from x/c of around 0.6 to 0.80 c. The experiments were carried out in the wind tunnel of the French-German Institute at St. Louis, which had a freestream turbulence intensity of 0.2%. The airfoil and velocity profiles and distributions of freestream velocity and skin-friction coefficient are shown in Figs. 13 and 14. As in Fig. 4, we can see a slightly slower calculated variation in freestream conditions between the x/c stations corresponding to laminar separation and turbulent reattachment which were reported to occur at 0.609 and 0.774 c, respectively. The velocity profiles imply separation at a similar location with reattachment slightly downstream of the measured value. The location of onset of transition was calculated at x/c of 0.71, which is consistent with an experimental measurement of maximum fluctuations in the near-wall region at the reattachment location of around 0.774. Figure 15 presents corresponding distributions of displacement thickness and shape factor which indicate close agreement between measurement and calculation except very close to the trailing edge.

The LNV109A airfoil is one of several proposed and examined by Liebeck and Camacho.[21] It is shown in Fig. 16 together

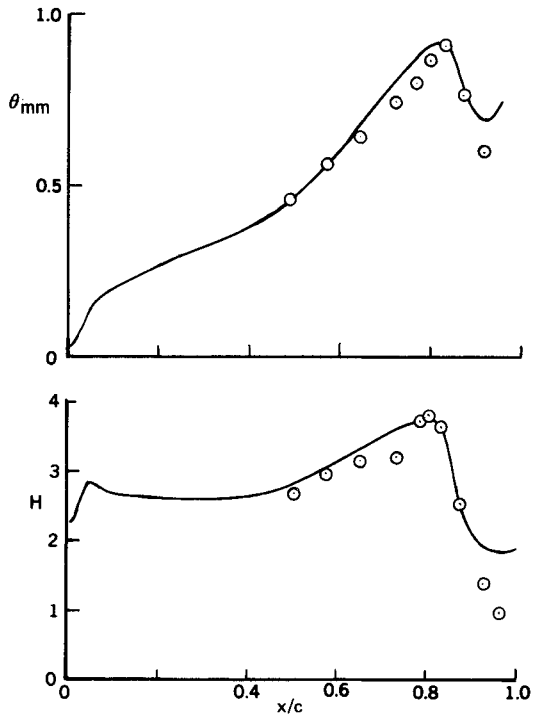

Fig. 12 Comparison of calculated (solid lines) and measured (symbols) momentum thickness θ and shape factor H values for the upper surface of the ONERA-D airfoil.

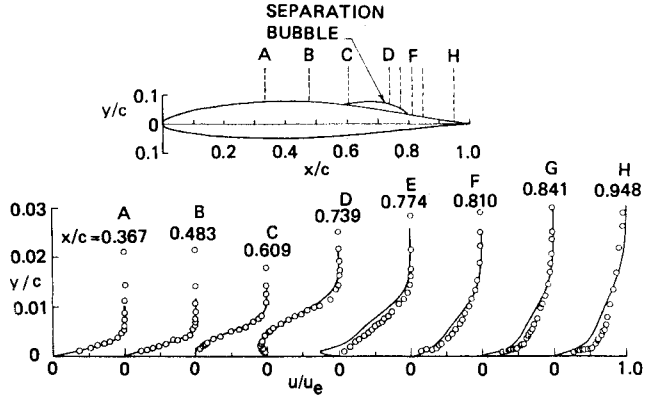

Fig. 13 Comparison of calculated (solid lines) and measured (symbols) velocity profiles for NACA 65-213 airfoil.

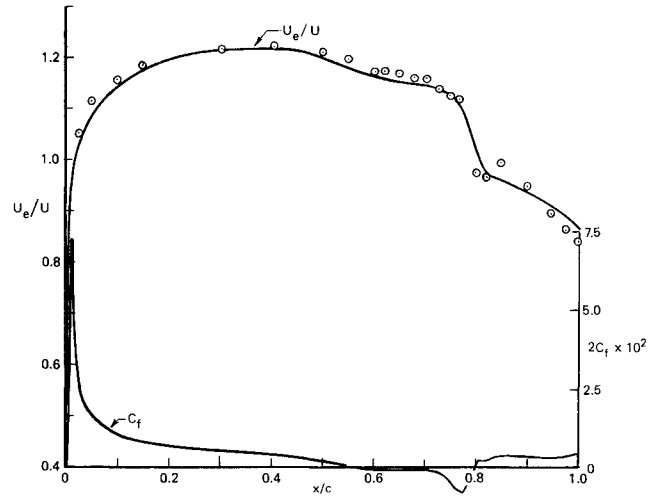

Fig. 14 Comparison of calculated (solid lines) and measured (symbols) freestream velocity and skin-friction for the NACA 65-213 airfoil.

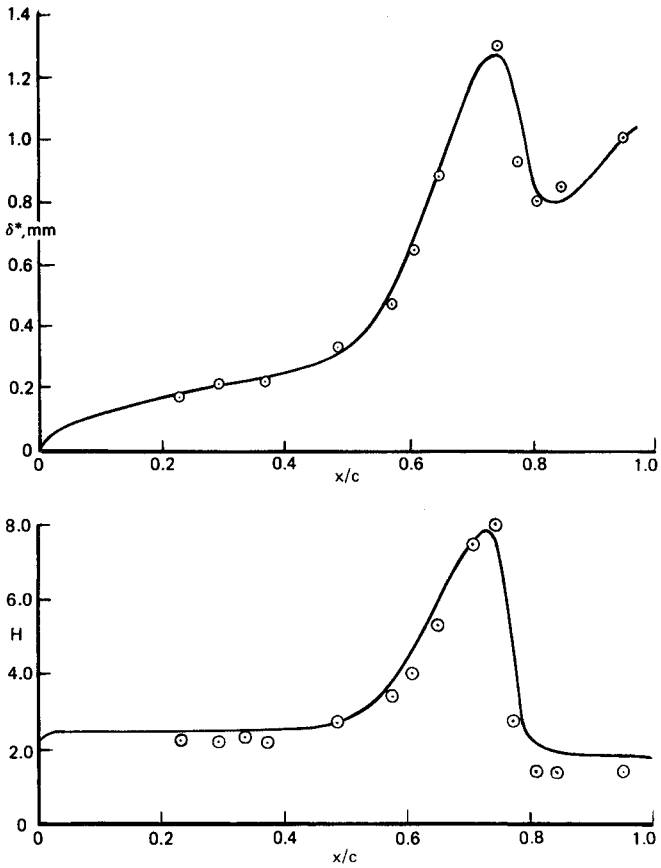

Fig. 15 Comparison of calculated (solid lines) and measured (symbols) displacement thickness δ^* and shape factor H for the NACA 65-213 airfoil.

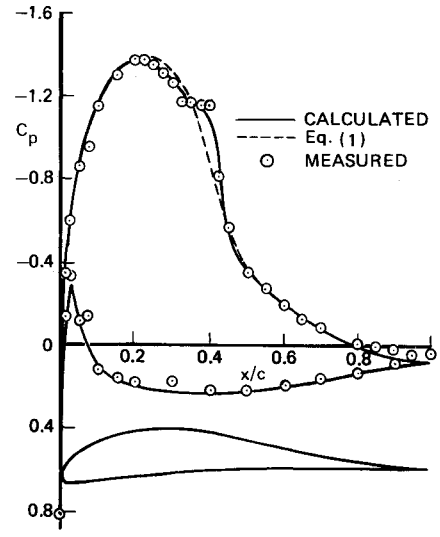

Fig. 16 Comparison of calculated and measured pressure coefficients for LNV109A airfoil[21], $R_c = 3.75 \times 10^5$.

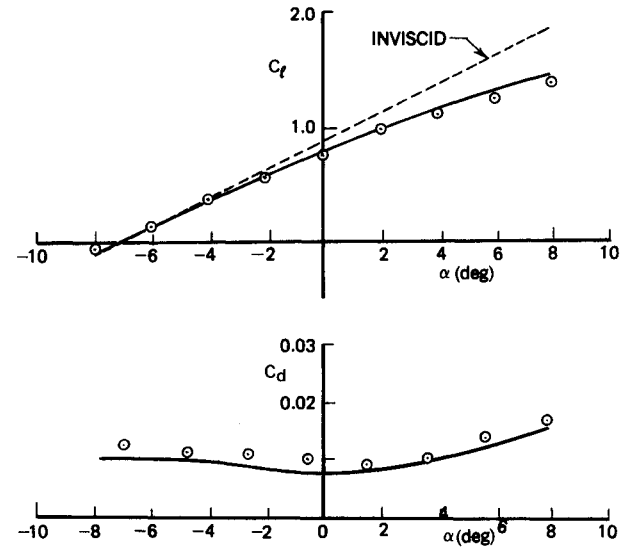

Fig. 18 Comparison of calculated (solid lines) and measured (symbols) for the Göttingen 797 airfoil, $R_c = 7 \times 10^5$.

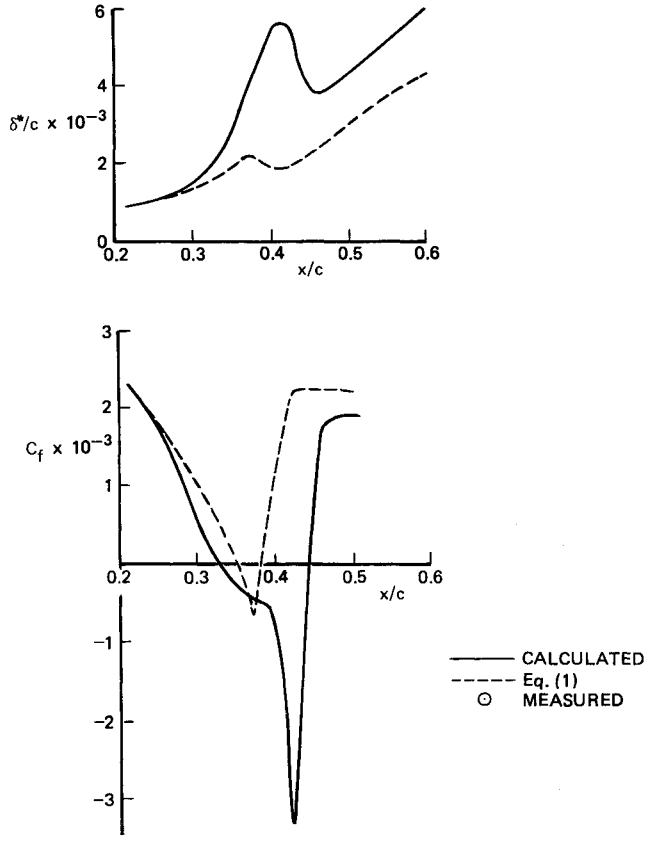

Fig. 17 Effect of transition location on the distribution of the local skin-friction coefficient and displacement thickness for the LNV109A airfoil.

Table 1 Lift and drag coefficients for LNV109A airfoil[21] at $\alpha = 3.415$

	C_ℓ	C_d	$(x/c)_{tr}$
Experiment	0.79	0.017	Not reported
Present method	0.79	0.015	0.385
Calculation with $(x/c)_{tr}$ from Eq. (1)	0.79	0.013	0.356

with the distribution of pressure coefficients obtained at a Reynolds number of 3.75×10^5 and an angle of attack of 3.415 deg. Figure 17 shows the effect of transition location on the distribution of local skin-friction coefficient and displacement thickness and Table 1 quantifies the effect upon lift and drag coefficients. With laminar flow imposed over the entire airfoil, the distribution of freestream velocity is very uniform from around 0.4 c, consistent with the near-zero, skin-friction coefficient. Transition to turbulent flow results in a separation bubble with consequent rise in freestream velocity and low but finite drag over the downstream half of the airfoil. The value of C_d obtained from the present calculation method is somewhat lower than the measured value but considerably better than the one in which transition was computed from Eq. (1).

The flow configurations of the preceding paragraphs involve low angle of attack with little wake effect and no upper-surface, trailing-edge separation. They represent, therefore, a limited range of flows that emphasize the effects of laminar separation bubbles and transition within them. In this respect, the evidence suggests that the calculation method performs well. The recent paper of Render et al.[22] describes results obtained with seven airfoils in the 8×6 ft wind tunnel at the Cranfield College of Aeronautics at Reynolds numbers from 3×10^5 to 1×10^6 and with angle of attack including those associated with stall. The models were "quasi-two-dimensional" in that there was a small gap at each end to allow direct measurements of force and this aspect together with tunnel blockage was carefully considered in analyzing the results. It can be expected that the size of the separation bubble associated with higher angles of attack will be much less than those of the previous paragraphs so that the determination of the onset of transition and the properties of the region of transitional flow will be more readily calculable. As a consequence, two of the flows examined in Ref. 22 are considered in the following paragraph and in terms of lift and drag coefficients only.

The results of two tests of the ability of the calculation to deal with the effect of angle of attack are shown in Figs. 18 and 19 where lift and drag coefficients are reported for the Göttingen 797 and NACA 64_3-418 airfoils, respectively, up to a maximum angle of 11 deg. In both cases, the measurements and calculations of C_ℓ are in excellent agreement up to and including stall, and the values of C_d are close to each other with a systematic error in the case of the NACA 64_3-418 airfoil. The

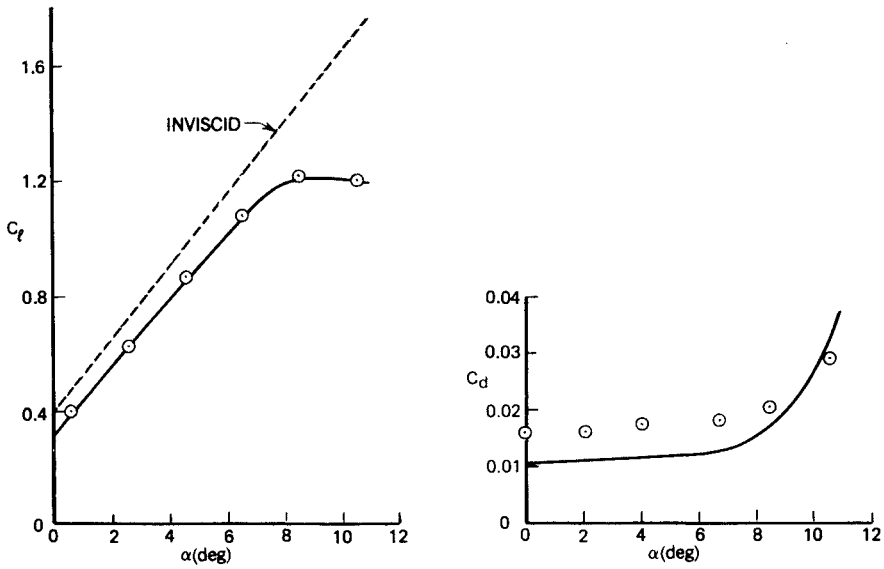

Fig. 19 Comparison of calculated (solid lines) and measured (symbols) results for the NACA 64_3-418 airfoil. $R_c = 3 \times 10^5$.

low values of drag coefficient in this last case are surprising particularly since the discrepancy between measurement and calculation is constant for angles of attack from 0–8 deg.

V. Concluding Remarks

It is evident from the preceding text that the successful calculation of low-Reynolds-number airfoil flows requires interaction between inviscid- and viscous-flow equations for a solution domain which, for higher angles of attack, encompasses the wake. Transition to turbulent flow must be correctly represented, and this can be achieved with a combination of the e^n method to determine the onset of transition, the algebraic, eddy-viscosity formulation of Cebeci and Smith, and a new correlation to represent the extent of the transition region. The calculation of transition must also be performed interactively to insure that the relationship between the location of transition and the extent of its influence are correctly represented.

With these ingredients, the method has been shown to calculate correctly the flow over a large number of airfoils, all of which involve regions of separation.

Acknowledgment

This research was sponsored by the Office of Naval Research under Contract N00014-85-K-0346.

References

[1]Halsey, N. D., "Potential Flow Analysis of Multielement Airfoils Using Conformal Mapping," *AIAA Journal,* Vol. 17, 1979, p. 1281.

[2]Cebeci, T. and Bradshaw, P., *Momentum Transfer in Boundary Layers,* McGraw-Hill/Hemisphere, Washington, DC, 1977.

[3]Cebeci, T., Clark, R. W., Chang, K. C., Halsey, N. D., and Lee, K., "Airfoils With Separation and the Resulting Wakes," *Journal of Fluid Mechanics,* Vol. 163, 1986, pp. 323–347.

[4]Michel, R., "Etude de la Transition sur les Profiles d'Aile; Establissement d'un Critère de Determination de Point de Transition et Calcul de la Trainee de Profile Incompressible," ONERA Rept. 1/1578A, 1951.

[5]Granville, P. S., "The Calculation of the Viscous Drag of Bodies of Revolution," David W. Taylor Model Basin Rept. 849, 1953.

[6]Horton, H. P., "A Semi-Empirical Theory for the Growth and Bursting of Laminar Separation Bubbles," Aeronautical Research Council CP 1073, 1967.

[7]Crimi, P. and Reeves, B. L., "Analysis of Leading-Edge Separation Bubbles on Airfoils, *AIAA Journal,* Vol. 24, 1976, pp. 1547–1555.

[8]Smith, A. M. O., "Transition, Pressure Gradient, and Stability Theory," *Proceedings of the IX International Congress of Applied Mechanics,* Vol. 4, 1956, pp. 234–244.

[9]Van Ingen, J. L., "A Suggested Semi-empirical Method for the Calculation of the Boundary-Layer Region," Delft, Holland, Rept. No. VTH71, VTH74, 1956.

[10]Mack, L. M., "Transition and Laminar Instability," Jet Propulsion Lab. Pub. 77-15, Pasadena, CA, 1977.

[11]Wazzan, A. R., "Spatial Stability of Tollmien-Schlichting Waves," *Progress in Aerospace Sciences,* Vol. 16, No. 2, 1975, pp. 99–127, Pergamon, New York, 1975.

[12]Nayfeh, A. H., Ragab, S. A., and Al-Maaitah, A., "Effect of Roughness on the Stability of Boundary Layers," AIAA Paper 86-1044, 1986.

[13]Fage, A., "The Smallest Size of Spanwise Surface Corrugation which Affects Boundary-Layer Transition on an Airfoil," Aeronautic Research Council, R&M 2120, Jan. 1943.

[14]Cebeci, T. and Egan, D., "Prediction of Transition Due to Isolated Roughness," *AIAA Journal,* Vol. 27, 1989, pp. 870–875.

[15]Cebeci, T. and Smith, A. M. O., *Analysis of Turbulent Boundary Layers,* Academic, New York, 1974.

[16]Chang, K. C., Bui, M. N., Cebeci, T., and Whitelaw, J. H., "The Calculation of Turbulent Wakes," *AIAA Journal,* Vol. 24, 1986, p. 200.

[17]Cebeci, T., Chang, K. C., Li, C., and Whitelaw, J. H., "Turbulence Models for Wall Boundary Layers," *AIAA Journal,* Vol. 24, 1986, pp. 359–360.

[18]Gault, D. E., "An Experimental Investigation of Regions of Separated Laminar Flow," NACA TN 3505, 1955.

[19]Cousteix, J. and Paihas, G., "Etude Exploratorie d'un Processus de Transition Laminaire-Turbulent au Voisinage du Decollemente d'un Couche Limite Laminaire," T.P. 1979-86; also, LeRecherche Aerospatiale No. 1979-3, pp. 213–218.

[20]Hoheisel, H., Hoeger, M., Meyer, P., and Koerber, G., "A Comparison of Laser-Doppler Anemometry and Probe Measurements within the Boundary Layer of an Airfoil at Subsonic Flow," *Laser Anemometry in Fluid Mechanics-II, Selected Papers from the Second International Symposium on Applications of Laser Anemometry to Fluid Mechanics,* July 1984, LADOAN, pp. 143–157.

[21]Liebeck, R. H. and Camacho, P. P., "Airfoil Design at Low Reynolds Number with Constrained Pitching Moment," *Proceedings of Conference on Low Reynolds Number Airfoil Aerodynamics,* edited by J. Mueller, University of Notre Dame, UNDAS-CP-77B123, Indiana, 1985, p. 27.

[22]Render, P. M., Stollery, J. L., and Williams, B. R., "Aerofoils at the Low Reynolds Number—Prediction and Experiment, *Numerical and Physical Aspects of Aerodynamic Flows III,* edited by T. Cebeci, Springer-Verlag, New York, 1986, pp. 155–167.

[23]Reyher, T. A. and Flügge-Lotz, I., "The Interaction of a Shock-Wave with a Laminar Boundary Layer," *International Journal of Nonlinear Mechanics,* Vol. 3, 1968, pp. 173–199.

[24]Veldman, A. E. P., "New Quasi-Simultaneous Method to Calculate Interacting Boundary Layers," *AIAA Journal,* Vol. 19, 1981, p. 769.

[25]Cebeci, T., Stewartson, K., and Williams, P. G., "Separation and Reattachment Near the Leading Edge of a Thin Airfoil at Incidence," AGARD CP-291, Paper 20, 1981.

[26]Chen, K. K. and Thyson, N. A., "Extension of Emmons' Spot Theory to Flows on Blunt Bodies," *AIAA Journal,* Vol. 9, 1971, pp. 821–825.

[27]Thompson, B. E. and Whitelaw, J. H., "Characteristics of a Trailing-Edge Flow with Turbulent Boundary-Layer Separation," *Journal of Fluid Mechanics,* Vol. 157, 1985, p. 305.

[28]Nakayama, A., "Characteristics of the Flow Around Conventional and Supercritical Airfoils," *Journal of Fluid Mechanics,* Vol. 160, 1985, p. 155.